Microbiology (2014), **160**, 2374–2386 **DOI** 10.1099/mic.0.078527-0

Editor's Choice

Anionic lipids and the cytoskeletal proteins MreB and RodZ define the spatio-temporal distribution and function of membrane stress controller PspA in *Escherichia coli*

Goran Jovanovic,[1] Parul Mehta,[1] Liming Ying[2] and Martin Buck[1]

[1]Department of Life Sciences, Imperial College London, London SW7 2AZ, UK

[2]National Heart and Lung Institute, Imperial College London, London SW7 2AZ, UK

Correspondence
Goran Jovanovic
g.jovanovic@imperial.ac.uk
Martin Buck
m.buck@imperial.ac.uk

Received 25 February 2014
Accepted 8 August 2014

All cell types must maintain the integrity of their membranes. The conserved bacterial membrane-associated protein PspA is a major effector acting upon extracytoplasmic stress and is implicated in protection of the inner membrane of pathogens, formation of biofilms and multi-drug-resistant persister cells. PspA and its homologues in Gram-positive bacteria and archaea protect the cell envelope whilst also supporting thylakoid biogenesis in cyanobacteria and higher plants.
In enterobacteria, PspA is a dual function protein negatively regulating the Psp system in the absence of stress and acting as an effector of membrane integrity upon stress. We show that in *Escherichia coli* the low-order oligomeric PspA regulatory complex associates with cardiolipin-rich, curved polar inner membrane regions. There, cardiolipin and the flotillin 1 homologue YqiK support the PspBC sensors in transducing a membrane stress signal to the PspA-PspF inhibitory complex. After stress perception, PspA high-order oligomeric effector complexes initially assemble in polar membrane regions. Subsequently, the discrete spatial distribution and dynamics of PspA effector(s) in lateral membrane regions depend on the actin homologue MreB and the peptidoglycan machinery protein RodZ. The consequences of loss of cytoplasmic membrane anionic lipids, MreB, RodZ and/or YqiK suggest that the mode of action of the PspA effector is closely associated with cell envelope organization.

INTRODUCTION

Maintaining membrane integrity is fundamental to all cell types and of key importance to energy production, signalling, adaptation to the environment and cellular compartmentalization. Many Gram-negative bacteria mount a major adaptive response to extracytoplasmic stress by inducing the phage shock protein (Psp) system (reviewed by Model *et al.*, 1997; Darwin, 2005; Joly *et al.*, 2010). Related stress control systems are found in Gram-positive bacteria, cyanobacteria, archaea and higher plants (Joly *et al.*, 2010).

The Psp system of Gram-negative bacteria is induced by a variety of membrane stress stimuli such as protein translocation defects (Joly *et al.*, 2010; Wang *et al.*, 2010; Wickström *et al.*, 2011) and production of secretins, e.g. phage f1 protein IV (pIV), PulD, YscC, OutD, which are components of the types II, III and IV secretion systems (reviewed by Joly *et al.*, 2010; Yamaguchi & Darwin, 2012). The Psp response of bacterial pathogens protects the cell envelope during infection and is important for biofilm formation and virulence whilst also being implicated in antibiotic resistance and formation of persister cells (reviewed by Joly *et al.*, 2010; Darwin, 2013; see also Dhamdhere & Zgurskaya, 2010; Vega *et al.*, 2013; Wallrodt *et al.*, 2014). Agents inducing *psp* impair the plasma membrane and dissipate the proton motive force (pmf). A drop in pmf may not be sufficient to induce the Psp response and multiple signals appear to be integrated to induce the response in enterobacteria (Wang *et al.*, 2010; Engl *et al.*, 2011). The highly conserved bacterial peripheral membrane protein PspA acts as a major effector that, through a yet unknown mechanism, repairs the membrane and so preserves the pmf (Joly *et al.*, 2010). Homologues of PspA in *Mycobacterium* and other Gram-positive bacteria (e.g. LiaH in *Bacillus*) have been postulated to maintain cell wall homeostasis upon extracytoplasmic stress (Joly *et al.*, 2010; White *et al.*, 2011; Darwin, 2013), to confer resistance to cell wall/peptidoglycan (PGL) and membrane integrity-targeting antibiotics (reviewed by Jordan *et al.*, 2008; Joly *et al.*, 2010). In cyanobacteria and plants, the PspA homologue VIPP1 is required for photosynthesis through support of thylakoid

Abbreviations: CL, cardiolipin; eGFP, enhanced green fluorescent protein; IM, inner membrane; PG, phosphatidylglycerol; PGL, peptidoglycan; pIV, phage f1 protein IV (secretin); pmf, proton motive force; Psp, phage shock protein; SMI, single molecule imaging; TIRF, total internal reflection fluorescence; V, Venus.

Supplementary Material is available with the online version of this paper.

membrane biogenesis and protection of the cell envelope (Westphal *et al.*, 2001; Aseeva *et al.*, 2004, 2007; Vothknecht *et al.*, 2012; Zhang *et al.*, 2012; Zhang & Sakamoto, 2013).

PspF, PspA, PspB and PspC are conserved in enterobacteria and constitute the core proteins of the Psp response (Huvet *et al.*, 2011). Under non-stress conditions in enterobacteria, σ^{54}-RNA polymerase-dependent *psp* expression is negatively regulated by PspA via its direct ~1 : 1 binding to the surface-exposed hydrophobic 'W56 loop' of the hexameric bacterial enhancer-binding protein PspF (Joly *et al.*, 2009; Zhang *et al.*, 2013). Under inner membrane (IM) stress, induction of *psp* involves the IM-bound PspB and PspC proteins sensing stress and recruiting the PspA-PspF inhibitory complex to the IM (Jovanovic *et al.*, 2010; Yamaguchi *et al.*, 2010). Relieving the inhibition of PspF imposed by PspA involves changing PspA's interacting partner from PspF to PspBC, resulting in strong induction of *psp* genes and formation of PspA effector complexes at the IM (Yamaguchi *et al.*, 2013; Mehta *et al.*, 2013). Upon stress, σ^{70}-controlled expression of PspF remains unchanged (Lloyd *et al.*, 2004).

Single molecule sensitivity imaging (SMI) studies of chromosome-expressed fluorescent fusion Venus–PspF (V–PspF) in live *Escherichia coli* cells established that PspF is predominantly hexameric and that the PspA-V–PspF nucleoid-bound inhibitory complex under non-stress conditions communicates with the IM in a PspA- and PspBC-dependent manner (Mehta *et al.*, 2013). Under IM stress, PspF is stably bound to the nucleoid and involved in transcription while V–PspA [or eGFP (enhanced green fluorescent protein)–PspA] is found within static polar and dynamic lateral IM complexes. Static polar IM complexes correlate with a PspA regulatory function within the signalling complex PspA-PspBC, while the dynamic lateral IM complexes correlate with PspA effector function (Engl *et al.*, 2009; Jovanovic *et al.*, 2014). When the dynamics of lateral membrane eGFP-PspA complexes are abolished or when PspA is mutated so it can interact with PspF and PspBC but cannot bind to the IM and form the lateral membrane complexes, it is able to form the polar IM complexes and respond to PspBC-dependent IM stress but is unable, for example, to conserve the pmf. The major oligomerization state of eGFP–PspA found in static polar foci is a 6-mer with a minority of additional high-order oligomers up to ~36-mer (Lenn *et al.*, 2011). Relief of negative control results in PspA binding to the IM, switch in oligomeric state from low-order to high-order oligomers and the appearance of lateral IM PspA effector complexes (Jovanovic *et al.*, 2014). These observations suggest that a switching mechanism linked to the stress signalling pathway in cellular polar membrane regions exists to convert PspA between its negative regulator (potentially 6-mer) and effector (36-mer) forms. Apparently, PspBC, as opposed to PspA, has a direct secretin-damage effector function in *Yersinia enterocolitica* (PspC has extra amino acids at its N terminus compared with the *E. coli* PspC) (Horstman & Darwin, 2012). Moreover, Yamaguchi *et al.* (2013) did not observe lateral IM PspA effector complexes upon stress, suggesting that the action of PspA effectors in stressed *Y. enterocolitica* cells might be orchestrated differently from that in *E. coli*. Nevertheless, at the same time it was established that the static polar PspBC sensor co-localizes with PspA at the onset of stress, consistent with the polar PspA-PspBC complex functioning in a regulatory manner in *E. coli*.

Impaired phospholipid biosynthesis is a strong inducer of PspA in *E. coli* (Bergler *et al.*, 1994). In turn, Kobayashi *et al.* (2007) provided evidence that the higher oligomeric form (36-mer) of purified PspA acts as an effector that binds phosphatidylglycerol (PG) and prevents proton leakage from membrane vesicles. In *E. coli*, the major phospholipid is phosphatidylethanolamine (~75 % of total IM lipids), which possesses a zwitterionic head group. The most abundant anionic IM phospholipids implicated in signalling and/or functioning of IM proteins are PG (~20 % of total IM lipids) and the dianion cardiolipin (CL) (~5 % of total IM lipids) (reviewed by Foss *et al.*, 2011). The polar and lateral regions of the IM are rich in PG whilst the majority of CL resides in polar regions (Foss *et al.*, 2011) (see Fig. S1a, available in the online Supplementary Material). Although PspA effector complexes do not directly bind CL *in vitro* (Kobayashi *et al.*, 2007), the position of the PspBC-dependent PspA regulatory complexes close to the poles implies that CL and/or negative curvature might be involved in localization and function of the PspBC sensor and/or a PspA-PspBC complex. Indeed, the function of, for example, the Tat protein translocation system is CL-dependent (reviewed by Arias-Cartin *et al.*, 2012; Berthelmann & Brüser, 2004), and PspBC-PspA–Tat direct interactions have been reported (Mehner *et al.*, 2012).

MreB is a bacterial actin and a key component of the bacterial cytoskeleton (reviewed by Typas *et al.*, 2012). The helix-like circumferential dynamics and function of the lateral IM PspA effector complexes depend on MreB in *E. coli* (Engl *et al.*, 2009). In *E. coli*, MreB assembles into short filaments that either bind directly to the cell membrane via its N-terminal amphipathic helix and move as independent units in directions that are perpendicular to the long axis of the cell (Salje *et al.*, 2011) or co-localize and interact with RodZ (van den Ent *et al.*, 2010) and organize the cell wall (PGL) synthesis machinery assembly, coupling their rotation in a helix-like circumferential fashion (van Teeffelen *et al.*, 2011) (see Fig. S1b). The PG-dependent lipid helices were observed in Gram-negative and Gram-positive bacteria (Barák *et al.*, 2008). Since PspA as an effector binds PG *in vitro* and PspA and PspB interact with MreB *in vivo* (Engl *et al.*, 2009), the spatial organization and dynamics of PspA, MreB and anionic lipids might be interlinked. These relationships could be important in response to physico-chemical changes of the IM relevant to regulation and functioning of the Psp system.

In this study we applied genetic tools in combination with SMI to explore *in vivo* how PspA communicates with the IM stress signalling pathways and undergoes a switch from

being a negative regulator to acting as an effector. We established a link between CL and induction of the Psp response on the one hand and the bacterial cytoskeleton and effector functions of PspA on the other. Our results provide evidence that membrane curvature, membrane lipid composition, bacterial actin MreB and cell wall biosynthesis machinery affect the dynamics of PspA upon IM stress.

METHODS

Bacterial strains, plasmids and growth conditions. Bacterial strains and plasmids used in this work are listed in Table S1. New strains were constructed using $P1_{vir}$ transduction (Miller, 1992) (e.g. MG1655 × MVA127 results in a strain MVA101; see Table S1). All strains were routinely grown under microaerobic conditions in Luria–Bertani (LB) broth or on LB agar plates at 37 °C (Miller, 1992). For microaerobic growth, overnight cultures of cells were diluted 100-fold (to OD_{600} ~0.025) and shaken in universals at 100 r.p.m. For SMI of eGFP–PspA and V–PspA, cells were grown in N^-C^- minimal medium supplemented with 0.4 % (w/v) glucose as carbon source, 10 mM NH_4Cl as nitrogen source, and trace elements at 30 °C as described previously (Engl *et al.*, 2009; Mehta *et al.*, 2013). The expression of pIV from pMJR129 was induced by 1 mM IPTG for 10 or 20 min. The expression from pCA24N-based constructs (JW plasmids, see Table S1) was induced by 0.1 mM IPTG for 1 h. The expression of eGFP–PspA and the expression of pIV from pGJ4 were leaky and constitutive. The antibiotics used were ampicillin (100 μg ml^{-1}), kanamycin (25 or 50 μg ml^{-1}, as indicated), chloramphenicol (30 μg ml^{-1}), tetracycline (10 μg ml^{-1}) and fosfomycin (16, 32 or 64 μg ml^{-1}, as indicated).

***In vivo* assays.** The activity of chromosomal transcription fusion F(*pspA–lacZ*) was measured using the β-galactosidase (β-Gal) assay as described by Miller (1992). For the β-Gal assay, overnight cultures grown at 37 °C were diluted 100-fold and grown under the same conditions until mid-exponential phase. The β-Gal data for all assays shown (except for the experiments with fosofomycin) are presented as the mean values (with SD error bars) of measurements of six samples (technical duplicates of three independently grown cultures of each strain).

For the experiment using fosfomycin, WT or WT + pIV cells were grown as above until mid-late-exponential phase and then each day culture was separated into five samples. The separate samples were inoculated with 0, 16 and 32 μg ml^{-1} (1 MIC, 64 μg ml^{-1}) fosfomycin, incubated for an additional 10 min at 37 °C and then assayed for β-Gal activity. The β-Gal data are presented for each of the three independent experiments.

The growth of WT and different mutants under non-stress or stress (pIV production) was measured in LB at 37 °C. The OD_{600} of overnight cultures was measured and culture densities were then standardized to OD_{600} 0.025 at $t=0$, after inoculation into 20 ml LB, and then shaken at 100 r.p.m. at 37 °C. The cells were taken for measurements of cell growth at OD_{600} and c.f.u. at hourly intervals (1–7 h). The data presented are from a single experiment in which all strains were tested simultaneously. The growth of a strain from three independent assays was compared with either an isogenic strain carrying the control vector plasmid or (for the mutants) with the WT parent strain before and after stress.

For cell growth and fosfomycin LacZ expression experiments, the statistical significance of differences between strains was determined using Students *t*-test. A *P* value less than 0.05 is considered to be significant.

Proteins. Expression of V–PspA and pIV was determined using antibodies against Venus [JL-8 Living Colours (Clonetech); 1 : 5000] and pIV (1 : 1000), respectively, and Western blotting. The Western blot analyses were performed on a Bench Pro 4100 Card processing station (Invitrogen). Proteins were detected using the ECL plus Western Blotting Detection kit (GE Healthcare) and images were visualized using the Bio-Rad GelDoc and ChemiDoc Imaging system with Image Lab software. The quantitative analyses were performed using ImageJ software.

Microscopy and imaging data analyses. Cells expressing plasmid-borne eGFP–PspA or chromosomal fusion of V–PspA were grown at 30 °C in minimal medium (see above). The live cells were immobilized on 1 % agarose pads set on a glass slide surface as described (Engl *et al.*, 2009). For the experiment where the V–PspA expression was analysed after 10 or 20 min induction of pIV, IPTG (1 mM final) was added directly to the agarose pads simultaneously with the cells. V–PspA was visualized using wide field epifluorescence microscopy. The expression of pIV was tested independently in the same samples grown in medium (0, 10 or 20 min) using Western blot and pIV antibodies (see above). For the experiment with fosfomycin, the stressed Δ*pspA* cells expressing V–PspA were grown to OD_{600} ~0.8, treated with 32 μg fosofomycin ml^{-1} for 10 min at 37 °C and imaged. The wide field or total internal reflection fluorescence (TIRF) SMI of live bacterial cells by means of a custom-built inverted epifluorescence/TIRF microscope based on a Nikon TE2000 optical system was as described (Mehta *et al.*, 2013). TIRF microscopy was employed to limit the laser penetration to up to ~50–100 nm into the bacterial cell in order to differentiate between nucleoid- and membrane-associated V–PspA foci. The axial resolution for wide field imaging is ~1 μm, so that an entire *E. coli* cell with diameter ~500 nm was imaged; hence the foci within the same/similar *Z* (e.g. nucleoid-associated and polar membrane) can be in focus. The exposure time was 38 ms (for eGFP) or 15 ms (for Venus). A 100–1000 frame video sequence with 2 × 2 binning at a frame interval of 25 ms (for eGFP) or 30 ms (for Venus) was recorded. The Deltavision OMX V3 system (Applied Precision) with 3 ms exposure time at a frame interval of 44 ms was used for photobleaching experiments of the rare V–PspA static foci observed in the nucleoid under non-stress conditions and of V–PspA foci at the poles under non-stress or stress conditions. Photobleaching traces of individual V–PspA static nucleoid foci under non-stress conditions and polar foci from non-stress and stressed cells were analysed and the oligomeric states were determined as described (Lenn *et al.*, 2011; Mehta *et al.*, 2013). The images were analysed using ImageJ (http://imagej.nih.gov/ij/) and FiJi. The quantitative analysis of localization of V–PspA foci in the cell, the quantification of number of foci per cell and the total raw intensity profiles were performed using ImageJ software. Cells expressing eGFP–PspA or V–PspA were analysed to determine the intensity of foci at specific cellular locations. For the spatial analysis of a signal, a line approximately 18 pixels wide was drawn along the longitudinal axis of cells of similar lengths to cover the entire cell, and the intensity values were obtained, yielding pixel-by-pixel intensity values across the cell length from pole to pole. When the differences in intensity values were high, for comparison we normalized the data points representing the mean intensity. The apparent 2D diffusion analysis (diffusion coefficient *D*) of V–PspA foci determined using Matlab (Mathwork) scripts was as described (Mehta *et al.*, 2013).

RESULTS

IM stress causes formation of V–PspA high-order oligomers in polar membrane regions and an increase of V–PspA complexes in lateral membrane regions

To assess and quantify the spatial and temporal dynamics of V–PspA under increasing IM stress conditions, we used

a strain lacking the native *pspA* gene and expressing chromosomal single-copy P_{pspA}-V–PspA (Mehta *et al.*, 2013; see also Fig. 1a) in the absence or presence of increasing amounts of pIV. pIV is an outer membrane secretin and its mislocalization into the IM induces the PspBC-dependent Psp response (Joly *et al.*, 2010). The V–PspA (or eGFP–PspA) fusion exhibits reduced (50 %) negative control activity compared with WT PspA (Engl *et al.*, 2009; Mehta *et al.*, 2013) and this accounts for the moderately elevated expression of both V–PspA and PspBC under non-stress conditions in a Δ*pspA* mutant (Jovanovic *et al.*, 2014). Consequently, in wide field SMI we observed V–PspA complexes (2 ± 0.3 foci per cell, $n=50$) in the polar region of the cell and some lateral membrane foci (Fig. 1b,Video S1). The pIV-induced IM stress and its time-dependent increase (Fig. 1f) led to a gradual elevation in total fluorescence intensity of V–PspA (Fig. 1g) and increased numbers of dynamic and static lateral V–PspA complexes (Fig. 1c, d, g, Videos S2 and S3). Notably, V–PspA expression, localization and dynamics in stressed cells closely resembled those of plasmid-borne eGFP–PspA as expressed in non-stressed Δ*pspA* cells (Fig. 1e, g, Video S4).

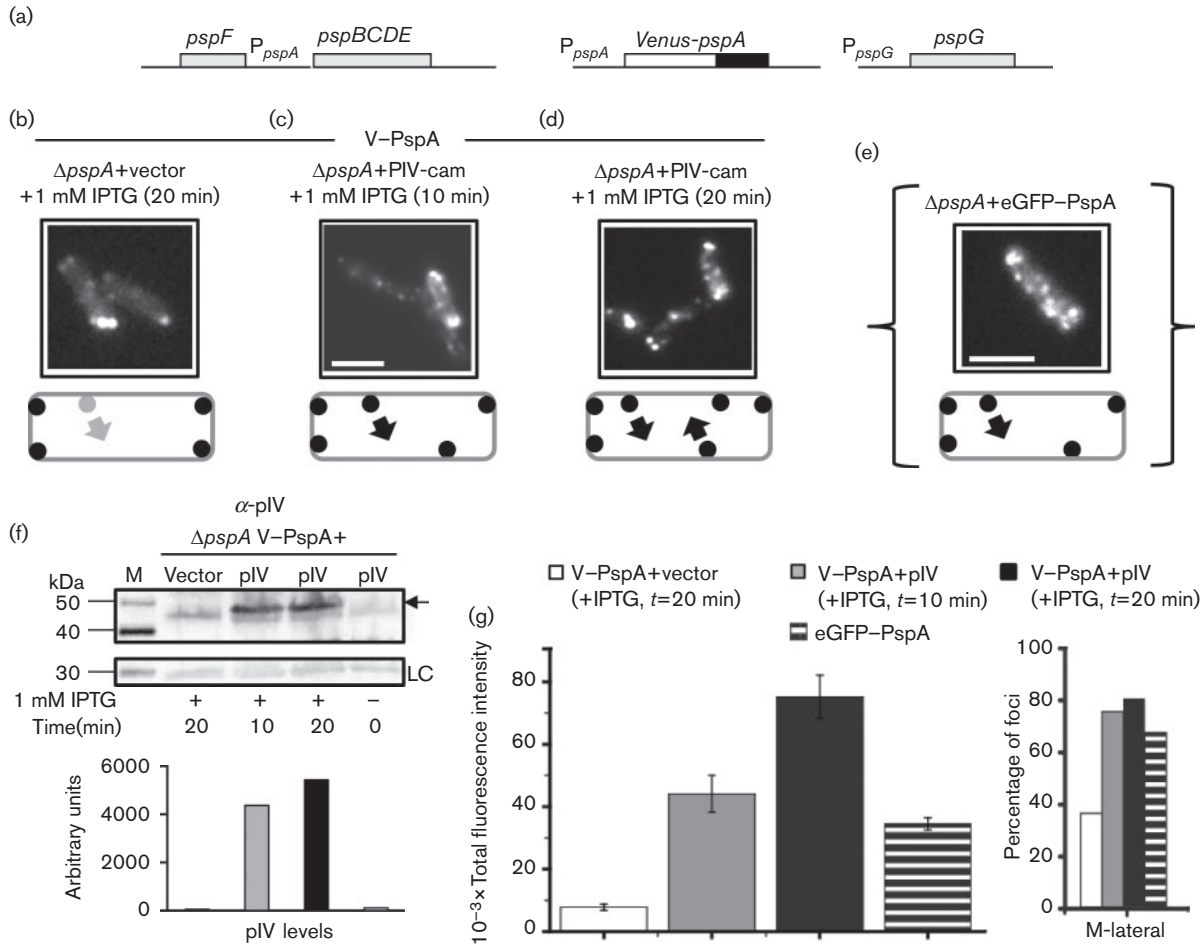

Fig. 1. The IM stress-dependent subcellular distribution of V–PspA. (a) Construct expressing chromosomal V–PspA under control of the *pspA* promoter (P_{pspA}) in a Δ*pspA* strain (MVA127). (b–d) Wide field SMI of MVA127 cells expressing V–PspA (white foci) in the absence of stress (+vector, pGZ119EH, after 20 min) (b) and upon stress (+pIV-cam, pMJR129) with pIV expression induced for 10 min (c) or for 20 min (d) before imaging. (e) Wide field SMI of eGFP–PspA (pEC1) in a non-stressed Δ*pspA* strain (MG1655Δ*pspA*). In (b–e) representative images are shown. Bars, 1 μm. Schematics represent non-quantitative interpretations of the images, depicting localizations and dynamics of V–PspA or eGFP–PspA: black dots, membrane foci; grey dot, less frequently observed membrane focus; arrows, dynamic membrane foci. (f) Western blot to show the level of pIV expression (band ~46 kDa) in cells from (c, d) and control pIV level in cells at 0 time point without IPTG (–). LC, loading control is the protein band from crude cell extract, which shows non-specific cross-reaction with the pIV antibody (α-pIV). M, molecular mass marker. Below: the quantification of pIV protein levels presented in arbitrary units. (g) Left: graph of total fluorescence intensity of V–PspA and eGFP–PspA foci ($n=50$) from (b–e). Error bars, ± SE. Right: *x*-axis, lateral membrane (M-lateral) localization of the V–PspA foci ($n=50$) from (b–d) and eGFP–PspA foci ($n=50$) from (e); *y*-axis, percentage of all foci analysed.

The total fluorescence intensity represents the number of V–PspA molecules. The very significant increase in total fluorescence intensity between 10 and 20 min induction of pIV (Fig. 1g, left) reflected a moderate increase in pIV level (Fig. 1f) and a small increase in the number of lateral V-PspA foci (10 min, 7 ± 0.6; 20 min, 8 ± 0.7; $n=50$) (see also Fig. 1g, right). However, the formation of foci containing high-order oligomeric V–PspA effectors may have been the main factor contributing to total fluorescence intensity.

Using wide field SMI and photobleaching we determined the oligomeric states of V–PspA under non-stress or stress growth conditions. In the non-stressed state V–PspA imaged as low-order (3–10-mer) assemblies in rare central static nucleoid-associated foci (Fig. 2a), presumably interacting with PspF and forming a PspA-PspF inhibitory complex at *psp* promoter(s) as shown by Mehta *et al.* (2013). This is in good agreement with *in vitro* data establishing that at least three PspA proteins are necessary to bind PspF for negative control (Zhang *et al.*, 2013). We also determined that in non-stressed cells V–PspA is a low-order assembly at polar foci, likely representing the PspA-PspBC membrane regulatory complex (Fig. 2b). During stress, the V–PspA in polar complexes was found as both low- (5- or 6-, up to 12-mer) and high-order assemblies (up to 25-mer; photobleaching and maturation of Venus fluorescence protein may limit the observed number of V–PspA subunits, especially in foci representing high-order oligomers) (Fig. 2b). It seems that the IM stress signals lead to a distinct dynamic response following an increase in V–PspA expression and its high-order oligomer assembly in polar membrane regions.

Efficient PspA-negative control is required for native basal level expression and spatial distribution of V–PspA

To determine the behaviour of V–PspA when expression of PspBC is natively controlled, the P_{pspA}-V–PspA was integrated as a single chromosomal copy into WT cells expressing native PspA (Fig. 3a). Normal regulation of *psp* expression, characterized by a low level of stable V–PspA, was observed under non-stress conditions whereas elevated levels were seen in pIV-stressed cells (Fig. 3b). When V–PspA and native PspBC were expressed at a basal level in non-stressed WT cells, V–PspA localized either as a single nearly static central nucleoid [by means of interacting with PspF (Mehta *et al.*, 2013; Jovanovic *et al.*, 2014); visible in wide field but not visible in TIRF] or as a static polar membrane complex (visible in both wide field and TIRF) (Fig. 3c). This is in agreement with V–PspF imaging in live cells revealing a single central nucleoid V–PspF-PspA inhibitory complex that communicates in a PspBC-dependent fashion with the polar membrane region by fast relatively free diffusion (Mehta *et al.*, 2013). Under stress, when expression of V–PspA is induced, we observed polar regulatory complexes and the appearance of static and dynamic lateral effector V–PspA complexes (Fig. 3d, Video S5). Therefore, with the negative control imposed by native PspA we could clearly visualize V–PspA exhibiting the 'off' and 'on' states of the Psp response.

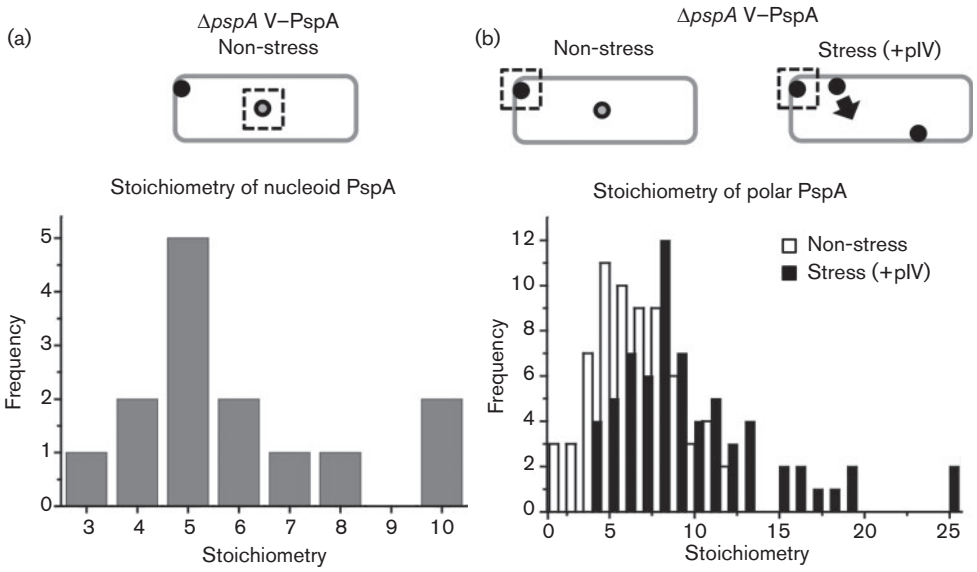

Fig. 2. The stoichiometry of V–PspA before and after IM stress. The stoichiometry was determined by photobleaching the V–PspA in MVA127 cells. The distribution of stoichiometries was calculated from data obtained for V–PspA. (a) Nucleoid-associated foci (non-stress, $n=14$) and (b) polar IM-associated foci under non-stress ($n=66$) or stress (+pIV, pGJ4; $n=67$) conditions. Schematics (as in Fig. 1); circles, nucleoid-associated foci; black dots, membrane foci; arrow, dynamic membrane focus.

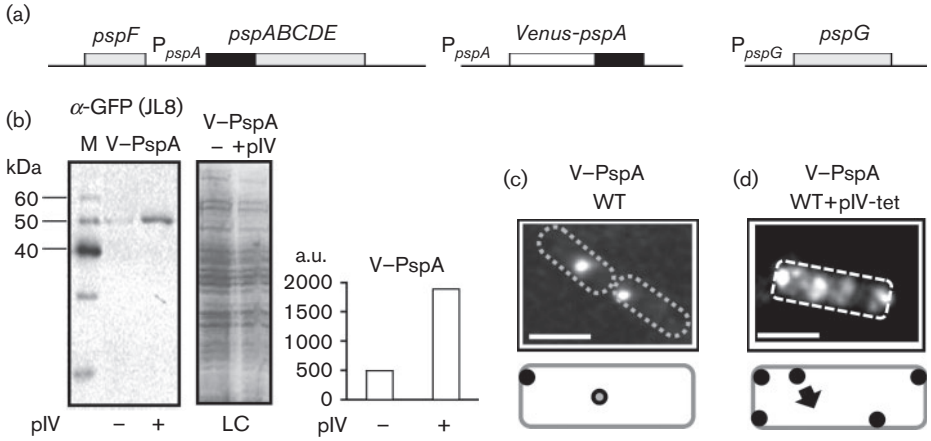

Fig. 3. The negative control of *psp* and spatial distribution of V–PspA. (a) Construct expressing chromosomal V–PspA under control of the *pspA* promoter (P_{pspA}) in *pspA*$^+$ cells (MVA101). (b) Left: Western blot to show the V–PspA fusion (~53 kDa) stability and expression in MVA101 before and after stress (+pIV, pGJ4). α-GFP JL8, Venus antibody; M, molecular mass marker. Middle: LC, loading control, Coomassie-stained MVA101−/+pIV samples. Right: quantification of V–PspA protein expression presented in arbitrary units (a.u.). (c, d) Wide field SMI of non-stressed MVA101 cells expressing V–PspA (c) and with induced expression of V–PspA upon stress (+pIV, pGJ4) (d). Representative images are shown. Bars, 1 μm. Schematics (as in Fig. 1): circle, nucleoid-associated focus; black dots, membrane foci; arrow, dynamic membrane focus.

CL is implicated in a PspBC-dependent induction of the Psp response

The anionic phospholipid CL has mainly a membrane curvature-associated polar localization (Renner & Weibel, 2011). PspA does not appear to bind membrane vesicles containing CL (Kobayashi *et al.*, 2007), but PspA is tethered by and co-localizes with static PspBC foci in curved polar membrane regions (Yamaguchi *et al.*, 2013; Mehta *et al.*, 2013). This suggests that localization of the inhibitory PspA-PspF complex or PspA within the PspA-PspBC regulatory complex at the poles of cells may depend on PspA interacting with the PspBC bound to CL-rich membrane domains. We examined the contribution of CL to PspA activities and to cell growth under IM stress in a Δ*cls* mutant (non-polar mutation) containing a significantly reduced amount of CL (Tan *et al.*, 2012).

We determined that the Δ*cls* mutation does not induce the Psp response per se and decreases basal level expression or induction of *pspA* under stress (Fig. 4a). In addition, the induction of *pspA* under stress is to some extent PspBC-independent in a Δ*cls* mutant (Fig. 4a). In the absence of negative control, in Δ*pspA* cells the Δ*cls* mutation did not impact on σ^{54}-dependent transcription of the *pspA* gene (Fig. S2a), suggesting that observed differences in *pspA* expression in Δ*cls* mutants reflect a change in the PspA negative control function. Additionally, the overexpression of either PgsA, implicated in biosynthesis of PG and CL or Cls, required for CL biosynthesis, did not induce the Psp response (Fig. S2b). We note that overexpression of phospholipid synthases had little impact on the overall pool of individual phospholipids within *E. coli* (reviewed by Raetz, 1986).

Growth in a stressed Δ*cls* mutant was delayed but the final growth yield was not significantly reduced compared with WT cells (Fig. 4b). As a control, a Δ*pspF* mutant lacking any induction of the Psp response exhibited growth that was severely impaired (Fig. 4c). Notably, the increased amount of PG seen in a Δ*cls* mutant (Tan *et al.*, 2012) and the fact that PspA effectors bind PG may account for cell adaptation and normal growth upon IM stress, even though the induction of the Psp response is decreased in Δ*cls* mutants.

To determine whether CL affects the subcellular localization of V-PspA, we imaged V-PspA in an *E. coli* Δ*cls* mutant background under non-stress or stress conditions using the wide field and TIRF modes of SMI. The majority of non-stressed Δ*cls* mutants showed only nucleoid-associated V–PspA (100 %, n=50, of mostly central foci not visible in TIRF) and no polar regulatory complexes (Fig. 4d), in agreement with increased negative control of PspF (Fig. 4a). Under stress, in Δ*cls* mutants we observed the appearance of lateral V–PspA foci but the number of polar complexes was significantly reduced compared with the WT (Figs 4e, g and S3a, b, Video S6). The total intensity of V–PspA foci in stressed Δ*cls* cells (Fig. S3c) correlated well with the level of *pspA* induction upon stress (Fig. 4a) and the amount of effector complexes was in accordance with their growth being similar to WT (Fig. 4b). As seen for the PspBC- and CL-independent induction of *pspA* (Fig. 4a), in stressed Δ*pspBC* Δ*cls* mutants the expression of V-PspA is induced and the formation of the lateral effector but not polar complexes can be readily observed (Fig. 4f).

Although we failed to construct a stable and functional PspB– or PspC–eGFP/Venus fusion protein to directly

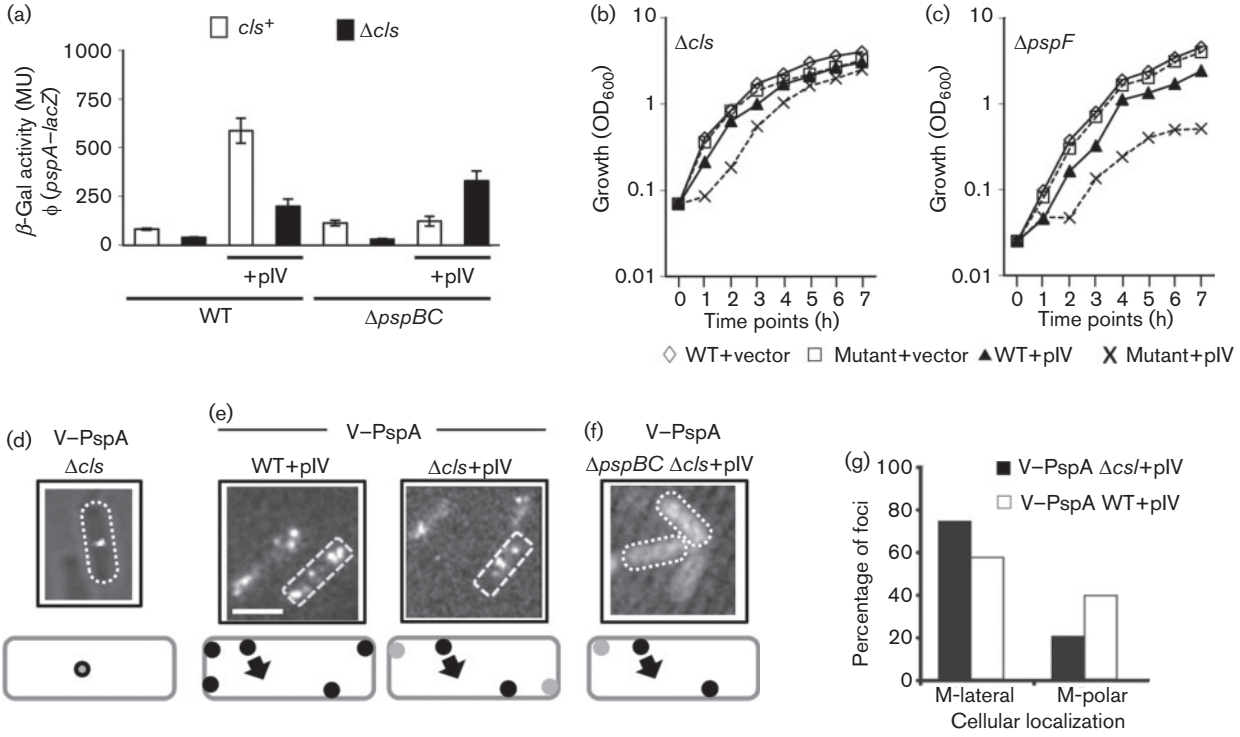

Fig. 4. CL as a determinant in IM stress signalling to PspA. (a) The activity of P_{pspA} in WT (MVA44), Δ*pspBC* (MVA45), Δ*cls* (MVA116) and Δ*pspBC* Δ*cls* (MVA117) cells under non-stress (vector pBR325D) or stress (+pIV, pGJ4) conditions. Error bars, ±SD. (b) Growth of the WT (MG1655) and Δ*cls* (MVA115) cells under non-stress (+vector) or stress (+pIV) conditions. (c) Growth of the Δ*pspF* mutant (MG1655Δ*pspF*) under non-stress or stress conditions as in (b). The experiments in (b) and (c) were done in triplicate and representative results are presented. Growth of Δ*cls*+pIV and Δ*pspF*+pIV was significantly different from corresponding non-stressed or WT non-stressed or stressed cells (for Δ*cls*+pIV, $P<0.001$; for Δ*pspF*+pIV, $P<0.02$) as determined by one sample *t*-test analysis of OD values. (d–f) Wide field SMI of V-PspA expressed in Δ*cls* (MVA118) in the absence of pIV (loss of polar foci) (d), in WT (MVA101) and Δ*cls* under stress (+pIV) (note loss of polar foci) (e), and in Δ*pspBC* Δ*cls* (MVA119) under stress (+pIV) (f). Representative images are shown. Bar, 1 μm. Schematics (as in Fig. 1): circle, nucleoid-associated focus; black dots, membrane foci; grey dots, less frequently observed membrane foci; arrows, dynamic membrane foci. (g) Subcellular localizations of the V–PspA foci from (e) are shown on the *x*-axis (M-lateral, lateral membrane; M-polar, polar membrane region) and percentage of all foci analysed ($n=115$ for WT+pIV, Δ*cls*+pIV) on the *y*-axis.

localize the Psp sensor(s) in a WT or *cls* mutant, it has been established that PspBC recruits the PspA-V-PspF complex to the IM in *E. coli* and co-localizes with PspA in the polar membrane regions of *Y. enterocolitica* cells (Yamaguchi *et al.*, 2013). Therefore, our results strongly suggest that the PspBC-dependent induction of the Psp response under stress and the localization of V–PspA within polar IM regulatory complexes are influenced by the presence of CL.

Apparently, CL depletion affects the membrane in numerous ways (reviewed by Arias-Cartin *et al.*, 2012) and could therefore indirectly influence PspB and PspC activity. Relevant to the Psp response, CL-associated flotillin YuaG (FloT) from *Bacillus subtilis* functionally organizes the bacterial membrane and interacts with proteins involved in membrane-related signalling and protein secretion (Donovan & Bramkamp 2009; Bach & Bramkamp, 2013). However, the PspA homologue LiaH or its regulator(s) has not been found to interact with YuaG. Intriguingly, there is a potential flotillin 1 homologue in *E. coli*, an IM protein YqiK, which might act in scaffolding of detergent-resistant microdomains under specific stress conditions (Hinderhofer *et al.*, 2009; López & Kolter, 2010). Therefore, to expand upon our results with CL, we assessed the contribution of YqiK to the induction, function and spatial organization of the Psp proteins. Lack of YqiK (Δ*yqiK*; non-polar mutation) did not induce *pspA* per se (Fig. S4a) but, although with less pronounced effect, reduced the level of induction of *pspA*, as also seen in a Δ*cls* mutant (Fig. S4a). As a control, we showed that the *yqiK* mutation did not impact on deregulated PspF-dependent transcription of *pspA* (Fig. S2a) and the overexpression of YqiK did not induce *pspA* (Fig. S2b). In line with the morphology of cells expressing YqiK and localization of YqiK-YFP in *E. coli* (López & Kolter, 2010),

our imaging results showed that overexpression of YqiK-GFP yielded enlarged cells and displayed IM localizations in distinct, relatively static (only local movement was seen) complexes in polar and lateral regions of the cell (Fig. S4c, d). The growth of Δ*yqiK* under stress was not substantially different from WT (Fig. S4b). The same was true for subcellular localization of V-PspA (Fig. S4e, Video S7). Hence, there are similarities between *cls* and *yqiK* mutants and it seems that YqiK supports signalling for the induction of the Psp response.

RodZ affects the Psp response and membrane localization of V-PspA

The effector function, lateral membrane localization and dynamics of PspA depend on MreB, while the induction of the Psp response and localization of PspA regulatory complexes are MreB independent (Engl *et al.*, 2009). MreB's circumferential movement along the long axis of the cell is driven by the process of PGL biosynthesis itself (White *et al.*, 2010; van Teeffelen *et al.*, 2011; Kawai *et al.*, 2011; Garner *et al.*, 2011; Domínguez-Escobar *et al.*, 2011; Olshausen *et al.*, 2013), and the association of MreB with the cell wall biosynthesis apparatus is via RodZ protein (Bendezú *et al.*, 2009; van den Ent *et al.*, 2010).

To address the potential link between PspA and RodZ (via MreB), we assayed activities and spatial distribution of PspA in *rodZ* mutants (Δ*rodZ*, non-polar mutation). We established that the absence of RodZ does not in itself induce *pspA* expression but allows a strong induction of *pspA* upon IM stress, which notably is PspBC-independent (Fig. 5a). As controls, lack of RodZ did not influence the PspF-dependent transcription of *pspA* (Fig. S2a) and overexpression of RodZ did not induce *pspA* (Fig. S2b). However, despite the induction of *pspA* under IM stress being elevated in a Δ*rodZ* mutant, the growth was impaired to an extent seen for the cells lacking a Psp response (Fig. 5b; and see Fig. 4c).

In Δ*rodZ* mutants with no rod-shaped morphology, it was hard to observe distinct V–PspA foci in the absence of IM stress (Fig. 5c). Under stress, the V–PspA expression was induced in Δ*rodZ* cells and we observed distinct dynamic effector complexes (Fig. 5d, Video S8). The same was true for plasmid-borne eGFP–PspA (Fig. 5e). The movement of eGFP–PspA in Δ*rodZ* mutants remained MreB-dependent since in the double Δ*mreB* Δ*rodZ* mutant the eGFP–PspA foci were static (Fig. 5f). However, RodZ did contribute to MreB-dependent spatial distribution of eGFP–PspA, which may be of importance for the function of the PspA effectors in WT cells. In the Δ*mreB* mutant, eGFP–PspA formed distinct static membrane foci (Engl *et al.*, 2009; see Fig. S5a) while in the double Δ*mreB* Δ*rodZ* mutant the eGFP–PspA foci localized in one membrane macro-domain (Figs 5f and S5b). Similarly, the eGFP–PspA foci in a Δ*mreB* Δ*yqiK* double mutant, lacking MreB and potential flotillin, localized in one static horseshoe-shaped macro-feature (Fig. S5c, d), suggesting MreB, RodZ and YqiK may be involved in organizing membrane regions for the intrinsic interactions of PspA complexes with the IM. Interestingly, in plant cells the Vipp1 homologue of PspA was very dynamic under osmotic stress and formed lateral membrane filament-like structures (Zhang *et al.*, 2012) resembling those of eGFP–PspA in Δ*mreB* Δ*rodZ* and Δ*mreB* Δ*yqiK* mutants.

Notably, even when the cell shape was perturbed, gross regulation of *pspA* transcription was retained. It appears that, so long as PspA can localize at the IM, then negative control can be relieved. V–PspA expression was induced by IM stress in Δ*pspBC* Δ*rodZ* cells (Fig. 5g; see also Fig. 5a). Even though the *rodZ* mutants do not have conventional polar membrane regions, the action of PspBC seems to be critical for V–PspA IM localization since the absence of PspBC in Δ*rodZ* mutants caused complete alteration of IM localization of V–PspA effector complexes. V–PspA then mainly decorated the entire IM (Fig. 5g), suggesting an additional role of PspBC in organizing some PspA effector complexes at the IM. Something similar has been observed in cells expressing the eGFP–PspA$_{\Delta 25-40}$ variant, with diminished interaction with PspBC (Jovanovic *et al.*, 2014). The resulting disorganization of the PspA effector that we saw here in the complete absence of PspBC and when the cell shape was perturbed was even more pronounced.

Block in cell wall synthesis elevates the Psp response to the IM stress and changes dynamics of the lateral membrane PspA effectors

To address whether a block in PGL synthesis directly affects the Psp response, we treated unstressed or stressed WT cells with different sublethal doses of fosfomycin to inhibit bacterial cell wall biogenesis by inactivating the cytoplasmic enzyme MurA that catalyses the first essential step in PGL biosynthesis (Brown *et al.*, 1995). We showed that a short (10 min) incubation with fosfomycin at 0.25 or 0.5 MIC increased the basal level transcription and pIV-dependent stress induction of *pspA* (Fig. 6a). Notably, the corresponding growth of non-stressed cells was better than that of the stressed cells (Fig. 6a). It appears that defective PGL biosynthesis causes an additional IM stress and this may correspondingly account for a Δ*rodZ* mutant elevating the Psp response to pIV (see Figs 5a and 6a).

To assess the localization and dynamics of the V–PspA effectors in stressed WT cells in the presence of fosfomycin, we used wide field SMI. Potentially, a block in PGL biosynthesis could lead to stalling of the membrane V–PspA effectors if their movement is tightly and solely coupled to the cell wall synthesis dynamics via RodZ and MreB. The observed RodZ-independent dynamics of V–PspA and eGFP–PspA (Fig. 5d, e) and MreB-dependent movement of eGFP–PspA (Fig. S5a) suggest that the subpopulation of V–PspA should not be affected. Counterintuitively, fosfomycin treatment (0.5 MIC, see above) sped up the diffusion of V–PspA in Δ*pspA* mutants producing pIV (mean D=0.02 μm^2 s^{-1}) compared with untreated stressed cells (mean D=0.01 μm^2 s^{-1}) (Fig. 6b). The

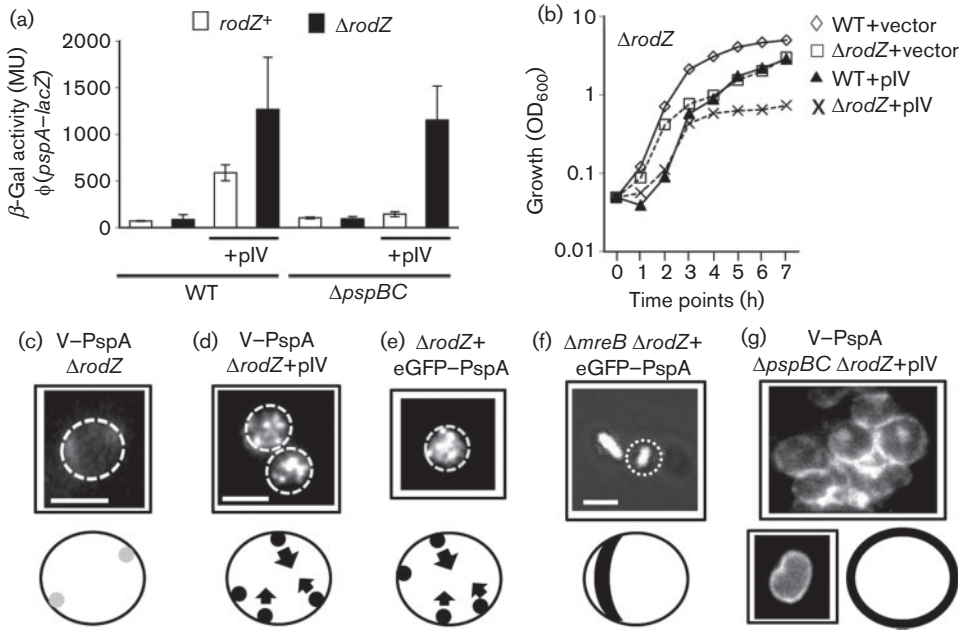

Fig. 5. Expression, localization and effector function of PspA in *rodZ* mutants. (a) The expression of P_{pspA} under non-stress (vector pBR325D) or stress (+pIV, pGJ4) conditions measured in WT (MVA44), Δ*pspBC* (MVA45), Δ*rodZ* (MVA108) and Δ*pspBC* Δ*rodZ* (MVA109) cells. Error bars, ±SD. (b) Growth of the WT (MG1655) and Δ*rodZ* mutant (MVA105) under non-stress (+vector) and stress (+pIV) conditions (the experiment was done in triplicate; a representative result is presented). Growth of Δ*rodZ*+pIV is significantly different from corresponding non-stressed or WT non-stressed or stressed strains ($P<0.04$) as determined by one sample *t*-test analysis of OD values. (c, d) Wide field SMI of V-PspA expressed in a Δ*rodZ* (MVA110) strain under non-stress (c) or stress (+pIV) (d) conditions. (e) The localization of eGFP-PspA (pEC1) in Δ*rodZ* (MVA105) cells resembles V–PspA+pIV localization and dynamics in Δ*rodZ* [in (d)]. (f) The localization and dynamics of eGFP–PspA in Δ*rodZ* are MreB-dependent. (g) Images of V–PspA in Δ*pspBC* Δ*rodZ* (MVA111) cells upon stress (+pIV; note decoration of the IM with the V–PspA). In (c–g) representative images are shown. Bars, 1 μm. Schematics (as in Fig. 1): black dots, membrane foci; grey dots, less frequently observed membrane foci; arrows, dynamic membrane foci; black shapes, foci arranged in macro-domain; black circles, foci decorate the membrane.

images show a mixture of cells with normal and more rounded shape (Fig. 6c) found to exhibit 9 ± 0.3 ($n=50$) V–PspA foci per cell. It is possible PspA became less constrained in its lateral membrane movements upon blocking of PGL synthesis.

DISCUSSION

Peripheral IM-binding proteins are emerging as providing important examples of where their localization and hence functionalities are directly sensitive to membrane phospholipid composition, membrane curvature and the bacterial cytoskeleton (Foss *et al.*, 2011). Here, we establish the functional relationships and interdependences between Psp response, bacterial membrane and cytoskeletal elements to provide insights into how cell structure relates to the perception and management of IM stress by PspA.

The IM stress induces strong *psp* expression, and consequently we see the formation of high-order oligomeric PspA effectors in polar regions together with an increase of PspA lateral effector complexes (Fig. S6). Potentially, the level of the signal and corresponding induction of PspA expression correlate with the strength of stimulus and thus also membrane damage. There is growing evidence that the integration of several signals induces the Psp response. Changes in membrane potential leading to a drop in pmf, as well as changes in redox state or mode of respiration were found to be either conditional or insufficient to signal the IM damage (Jovanovic *et al.*, 2009; Wang *et al.*, 2010; Engl *et al.*, 2011). Particular changes in properties of the membrane are likely to contribute to the origin of the IM stress signal(s) and the sites of PspA effector action. It is clear that there are at least two different pathways involved in IM stress signalling to PspA. One mode employs signal transduction to the PspA-PspF inhibitory complexes via PspBC sensors and the other acts through direct binding of PspA-PspF to a stress-related IM determinant (Fig. S6). Dual control of the σ^E regulon, which responds to outer-membrane stress (Lima *et al.*, 2013), has some similarity with the dual modes (PspBC-dependent and PspBC-independent) of IM binding of PspA upon stress.

Our results connect the CL-containing polar regions of the cell with the respective localizations of PspA and PspBC,

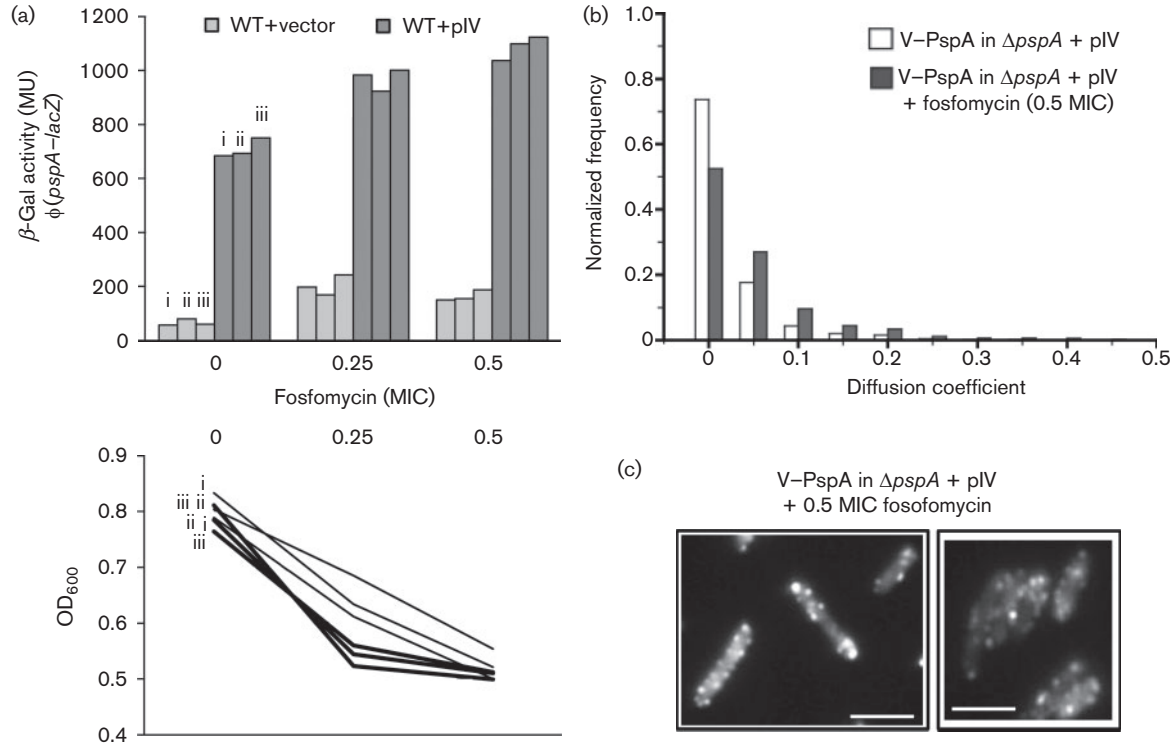

Fig. 6. Fosfomycin treatment increases IM stress and dynamics of V–PspA. (a) The expression of P_{pspA} was determined in three independent experiments (i–iii) in WT + vector (MVA44 + pBR325D, pale grey bars) and stressed WT + pIV (MVA44 + pGJ4, dark grey bars) cells in the absence (0) or presence of fosfomycin at different concentrations (1 MIC = 64 μg ml^{-1}) (see Methods for details). The expression of *pspA* in non-stressed or stressed cells treated with fosfomycin is significantly different from untreated cells (non-stressed, $P<0.01$; stressed, $P<0.005$) as determined by one sample *t*-test analysis of β-galactosidase activity. The line graph below shows the corresponding OD values of non-stressed (i–iii, thin lines) and stressed (i–iii, bold lines) cells in the absence or presence of fosfomycin. (b) The distribution of diffusion coefficients for V–PspA in Δ*pspA* cells (MVA127) under stress (+pIV, pGJ4) and in the absence (white bars, $n=709$) or presence (grey bars, $n=1106$) of 32 μg fosfomycin ml^{-1} (0.5 MIC) after 10 min of growth. The data are presented as normalized distributions of the diffusion coefficients (μm^2 s^{-1}) obtained as described by Mehta *et al.* (2013). (c) Example of wide field SMI of V–PspA in Δ*pspA* cells under stress and in the presence of fosfomycin as in (b). Bar, 1 μm.

PspBC signalling, IM binding of PspA and stress-dependent formation of the high-order oligomeric PspA effectors (Fig. S6). The PspBC sensors localized in polar regions transduce the IM stress signal(s) to the PspA-PspF inhibitory complex, releasing negative control of *psp*. PspC may sense a change in IM charge, membrane potential or curvature via CL, leading to a switch in PspC topology needed for recruiting PspA to the PspBC complex (Jovanovic *et al.*, 2010; Flores-Kim & Darwin, 2012) (see also Fig. S6). The protein Opi1 has been shown to exhibit similar behaviour, with its signalling dependent on intracellular pH and the protonation state of phosphatidic acid phosphate head groups (Young *et al.*, 2010), and Fis1 binding to lipid vesicles is increased upon protonation and concentration of anionic lipids (Wells & Hill, 2011). The PspBC complex may integrate the threshold level signals to modulate the Psp response to a range of stimuli. This can lead to reduction of noise and less pronounced oscillations of *psp* induction, in agreement with the mechanistic model of the Psp response (Toni *et al.*, 2011).

Our results also strongly suggest that upon stress in WT cells PspBC are also involved in connecting the PspA effector complex via MreB to particular cell features defined by RodZ, YqiK activities and anionic-lipid-rich membrane domains.

We showed here that the *psp* inducing pIV-originated signal(s), besides using the PspBC signalling pathway, can also act via a PspBC-independent mode. In addition, pIV production in a Δ*rodZ* background (or when PGL biogenesis is blocked) facilitates the IM stress and elevates the importance of the PspBC-independent response. Severe stresses, such as extreme osmotic shock, 50 °C heat shock, 10 % ethanol, have been shown to transiently induce *psp* in a PspBC-partial or -independent manner (reviewed by Model *et al.*, 1997). Therefore, extreme stimuli may cause PspA to bypass the PspBC signalling and directly respond to changes in the IM (see Fig. S6).

The several lines of evidence suggest that CL-associated protein translocation systems and adjacent PG-rich

domains might be targets for the PspA effector complexes positioned in polar IM regions of the cell (Fig. S6). Depletion or defects in all protein translocation systems (Sec, Tat, YidC, SRP) induce PspA (reviewed by Joly *et al.*, 2010). Importantly, a PspBC-dependent PspA–Tat interaction (Mehner *et al.*, 2012) suggests that the PspA effector function could involve direct repair of the CL-associated translocon system(s). The functions of PspA in repairing Tat defects can be substituted by Vipp1 in *E. coli*, while PspA partially substitutes for the same defect in the absence of Vipp1 (DeLisa *et al.*, 2004). Moreover, PspA stimulates protein export in *E. coli* (Kleerebezem & Tommassen, 1993) and a PspA homologue improves the pmf-dependent Tat- and Sec-supported heterologous protein secretion in *Streptomyces* (Vrancken *et al.*, 2007). As shown for PspA, the Tat and YidC homologues have been found in bacteria, archaea and chloroplasts. Clade PspA (CL0235) has two members, PspA/IM30 and Snf7. Snf7 is a family of proteins involved in protein sorting and transport from the endosome to the vacuole/lysosome in eukaryotic cells that play an important role in the degradation of both lipids and cellular proteins (Peck *et al.*, 2004). Therefore, one major and conserved function of PspA and its homologues may be to maintain the activities of protein translocation systems.

MreB defines the spatial distribution of lateral membrane PspA effectors and, together with its IM-binding partner RodZ, may be implicated in targeting cell wall synthesis machinery, conferring an adaptation of cells to IM stress (Fig. S6). Potentially, sites in lateral membrane regions where the cell wall synthesis machinery is assembled can be targeted by MreB-guided PspA effectors in order to support lipid II-dependent PGL biosynthesis and elongation of the lateral cell wall under IM stress. On that note, the expression of IM protein MurG, found to interact with MreB and to be essential for the lipid II-dependent cycle of PGL synthesis (see Fig. S1b), is upregulated in *E. coli* cells overexpressing PspA (Jovanovic *et al.*, 2006). In Gram-positive bacteria, lantibiotics and bacitracin interfere with cell wall synthesis by binding lipid II and strongly induce expression of the PspA homologue LiaH and its recruitment to membrane (Typas *et al.*, 2012; Domínguez-Escobar *et al.*, 2014). However, LiaH dynamics in *B. subtilis* were found to be independent of MreB and cell wall synthesis (Domínguez-Escobar *et al.*, 2014).

The cell wall synthesis machinery in *E. coli* may also serve to attract and functionalize the lateral membrane PspA effectors, leading to IM repair upon stress. Genomic analyses showed that RodZ function is conserved and unique to bacteria and that *rodZ* and *pgsA* (required for PG and CL biosynthesis) genes are often adjacent, suggesting they are functionally linked (Alyahya *et al.*, 2009). Note that PG has been found to directly bind PspA high-order oligomers which repair membrane damage *in vitro* (Kobayashi *et al.*, 2007). Also, gene-to-metabolite correlations suggest that in *E. coli* PG plays a critical role for membrane balance (Takahashi *et al.*, 2011). Notably, other envelope-associated complexes may well function through MreB and with changes in lipid organization impact upon the localization and dynamics of PspA.

Blocks in lipid biosynthesis induce the expression of PspA (Bergler *et al.*, 1994), suggesting that Psp through its effector function(s) may act to modulate lipid metabolism. As observed by using *pspA* or *pspG* mutants or overexpressing PspA or PspG (additional IM effector; Lloyd *et al.*, 2004; Jovanovic *et al.*, 2006; Engl *et al.*, 2009), these Psp effectors have the potential to diminish the expression of genes implicated in the glycerol shift and aerobic respiration and upregulate expression of genes that favour glycerol 3-phosphate conversion into phospholipids (Jovanovic *et al.*, 2006; Bury-Moné *et al.*, 2009). As we noted above, the increased amount of PG in the Δ*cls* mutant we used here may contribute to the IM stress adaptation when induction of Psp is reduced. Intriguingly, in *E. coli*, overexpression of the foreign protein MGS, which binds anionic lipids, greatly elevates PG production (Ariöz *et al.*, 2013), raising the possibility that the IM binding of highly expressed native PspA effectors may trigger a cellular signal for the stimulation of anionic lipid synthesis to repair and/or exchange PG (and CL).

In summary, the studies presented here show a functional link between CL, PspBC-dependent signalling and polar IM localization of PspA. Upon IM stress the PspA regulator switches to high-order oligomeric effector complexes in polar regions of the cell whilst employing bacterial actin MreB to target lateral membrane regions, some of which are marked by cell wall biosynthesis machinery protein RodZ. Further experiments are needed to reveal which properties of the IM change in a stress-specific manner to directly signal the membrane stress to PspA and to unravel the molecular mechanism of IM repair.

ACKNOWLEDGEMENTS

This work was funded by BBSRC and Leverhulme Trust project grants. We acknowledge A. Bruckbauer and A. Vaahtokari (London Research Institute, Cancer Research UK) for support at the SuperResolution Microscopy Core Facility, T. Lenn for technical help, Y.-L. Shih for MC1000 and MC1000 Δ*mreB* strains, and M. Russel for plasmid pMJR129. We thank J. Dworkin (Columbia University) for advice and members of the M. Buck laboratory for critical reading and comments on the manuscript.

REFERENCES

Alyahya, S. A., Alexander, R., Costa, T., Henriques, A. O., Emonet, T. & Jacobs-Wagner, C. (2009). RodZ, a component of the bacterial core morphogenic apparatus. *Proc Natl Acad Sci U S A* **106**, 1239–1244.

Arias-Cartin, R., Grimaldi, S., Arnoux, P., Guigliarelli, B. & Magalon, A. (2012). Cardiolipin binding in bacterial respiratory complexes: structural and functional implications. *Biochim Biophys Acta* **1817**, 1937–1949.

Ariöz, C., Ye, W., Bakali, A., Ge, C., Liebau, J., Götzke, H., Barth, A., Wieslander, Å. & Mäler, L. (2013). Anionic lipid binding to the

foreign protein MGS provides a tight coupling between phospholipid synthesis and protein overexpression in *Escherichia coli*. *Biochemistry* **52**, 5533–5544.

Aseeva, E., Ossenbühl, F., Eichacker, L. A., Wanner, G., Soll, J. & Vothknecht, U. C. (2004). Complex formation of Vipp1 depends on its α-helical PspA-like domain. *J Biol Chem* **279**, 35535–35541.

Aseeva, E., Ossenbühl, F., Sippel, C., Cho, W. K., Stein, B., Eichacker, L. A., Meurer, J., Wanner, G., Westhoff, P. & other authors (2007). Vipp1 is required for basic thylakoid membrane formation but not for the assembly of thylakoid protein complexes. *Plant Physiol Biochem* **45**, 119–128.

Bach, J. N. & Bramkamp, M. (2013). Flotillins functionally organize the bacterial membrane. *Mol Microbiol* **88**, 1205–1217.

Barák, I., Muchová, K., Wilkinson, A. J., O'Toole, P. J. & Pavlendová, N. (2008). Lipid spirals in *Bacillus subtilis* and their role in cell division. *Mol Microbiol* **68**, 1315–1327.

Bendezú, F. O., Hale, C. A., Bernhardt, T. G. & de Boer, P. A. (2009). RodZ (YfgA) is required for proper assembly of the MreB actin cytoskeleton and cell shape in *E. coli*. *EMBO J* **28**, 193–204.

Bergler, H., Abraham, D., Aschauer, H. & Turnowsky, F. (1994). Inhibition of lipid biosynthesis induces the expression of the *pspA* gene. *Microbiology* **140**, 1937–1944.

Berthelmann, F. & Brüser, T. (2004). Localization of the Tat translocon components in *Escherichia coli*. *FEBS Lett* **569**, 82–88.

Brown, E. D., Vivas, E. I., Walsh, C. T. & Kolter, R. (1995). MurA (MurZ), the enzyme that catalyzes the first committed step in peptidoglycan biosynthesis, is essential in *Escherichia coli*. *J Bacteriol* **177**, 4194–4197.

Bury-Moné, S., Nomane, Y., Reymond, N., Barbet, R., Jacquet, E., Imbeaud, S., Jacq, A. & Bouloc, P. (2009). Global analysis of extracytoplasmic stress signaling in *Escherichia coli*. *PLoS Genet* **5**, e1000651.

Darwin, A. J. (2005). The phage-shock-protein response. *Mol Microbiol* **57**, 621–628.

Darwin, A. J. (2013). Stress relief during host infection: the phage shock protein response supports bacterial virulence in various ways. *PLoS Pathog* **9**, e1003388.

DeLisa, M. P., Lee, P., Palmer, T. & Georgiou, G. (2004). Phage shock protein PspA of *Escherichia coli* relieves saturation of protein export via the Tat pathway. *J Bacteriol* **186**, 366–373.

Dhamdhere, G. & Zgurskaya, H. I. (2010). Metabolic shutdown in *Escherichia coli* cells lacking the outer membrane channel TolC. *Mol Microbiol* **77**, 743–754.

Domínguez-Escobar, J., Chastanet, A., Crevenna, A. H., Fromion, V., Wedlich-Söldner, R. & Carballido-López, R. (2011). Processive movement of MreB-associated cell wall biosynthetic complexes in bacteria. *Science* **333**, 225–228.

Domínguez-Escobar, J., Wolf, D., Fritz, G., Höfler, C., Wedlich-Söldner, R. & Mascher, T. (2014). Subcellular localization, interactions and dynamics of the phage-shock protein-like Lia response in *Bacillus subtilis*. *Mol Microbiol* **92**, 716–732.

Donovan, C. & Bramkamp, M. (2009). Characterization and subcellular localization of a bacterial flotillin homologue. *Microbiology* **155**, 1786–1799.

Engl, C., Jovanovic, G., Lloyd, L. J., Murray, H., Spitaler, M., Ying, L., Errington, J. & Buck, M. (2009). *In vivo* localizations of membrane stress controllers PspA and PspG in *Escherichia coli*. *Mol Microbiol* **73**, 382–396.

Engl, C., Beek, A. T., Bekker, M., de Mattos, J. T., Jovanovic, G. & Buck, M. (2011). Dissipation of proton motive force is not sufficient to induce the phage shock protein response in *Escherichia coli*. *Curr Microbiol* **62**, 1374–1385.

Flores-Kim, J. & Darwin, A. J. (2012). Phage shock protein C (PspC) of *Yersinia enterocolitica* is a polytopic membrane protein with implications for regulation of the Psp stress response. *J Bacteriol* **194**, 6548–6559.

Foss, M. H., Eun, Y.-J. & Weibel, D. B. (2011). Chemical-biological studies of subcellular organization in bacteria. *Biochemistry* **50**, 7719–7734.

Garner, E. C., Bernard, R., Wang, W., Zhuang, X., Rudner, D. Z. & Mitchison, T. (2011). Coupled, circumferential motions of the cell wall synthesis machinery and MreB filaments in *B. subtilis*. *Science* **333**, 222–225.

Hinderhofer, M., Walker, C. A., Friemel, A., Stuermer, C. A. O., Möller, H. M. & Reuter, A. (2009). Evolution of prokaryotic SPFH proteins. *BMC Evol Biol* **9**, 10.

Horstman, N. K. & Darwin, A. J. (2012). Phage shock proteins B and C prevent lethal cytoplasmic membrane permeability in *Yersinia enterocolitica*. *Mol Microbiol* **85**, 445–460.

Huvet, M., Toni, T., Sheng, X., Thorne, T., Jovanovic, G., Engl, C., Buck, M., Pinney, J. W. & Stumpf, M. P. H. (2011). The evolution of the phage shock protein response system: interplay between protein function, genomic organization, and system function. *Mol Biol Evol* **28**, 1141–1155.

Joly, N., Burrows, P. C., Engl, C., Jovanovic, G. & Buck, M. (2009). A lower-order oligomer form of phage shock protein A (PspA) stably associates with the hexameric AAA^+transcription activator protein PspF for negative regulation. *J Mol Biol* **394**, 764–775.

Joly, N., Engl, C., Jovanovic, G., Huvet, M., Toni, T., Sheng, X., Stumpf, M. P. H. & Buck, M. (2010). Managing membrane stress: the phage shock protein (Psp) response, from molecular mechanisms to physiology. *FEMS Microbiol Rev* **34**, 797–827.

Jordan, S., Hutchings, M. I. & Mascher, T. (2008). Cell envelope stress response in Gram-positive bacteria. *FEMS Microbiol Rev* **32**, 107–146.

Jovanovic, G., Lloyd, L. J., Stumpf, M. P. H., Mayhew, A. J. & Buck, M. (2006). Induction and function of the phage shock protein extracytoplasmic stress response in *Escherichia coli*. *J Biol Chem* **281**, 21147–21161.

Jovanovic, G., Engl, C. & Buck, M. (2009). Physical, functional and conditional interactions between ArcAB and phage shock proteins upon secretin-induced stress in *Escherichia coli*. *Mol Microbiol* **74**, 16–28.

Jovanovic, G., Engl, C., Mayhew, A. J., Burrows, P. C. & Buck, M. (2010). Properties of the phage-shock-protein (Psp) regulatory complex that govern signal transduction and induction of the Psp response in *Escherichia coli*. *Microbiology* **156**, 2920–2932.

Jovanovic, G., Mehta, P., McDonald, C., Davidson, A. C., Uzdavinys, P., Ying, L. & Buck, M. (2014). The N-terminal amphipathic helices determine regulatory and effector functions of phage shock protein A (PspA) in *Escherichia coli*. *J Mol Biol* **426**, 1498–1511.

Kawai, Y., Marles-Wright, J., Cleverley, R. M., Emmins, R., Ishikawa, S., Kuwano, M., Heinz, N., Bui, N. K., Hoyland, C. N. & other authors (2011). A widespread family of bacterial cell wall assembly proteins. *EMBO J* **30**, 4931–4941.

Kleerebezem, M. & Tommassen, J. (1993). Expression of the *pspA* gene stimulates efficient protein export in *Escherichia coli*. *Mol Microbiol* **7**, 947–956.

Kobayashi, R., Suzuki, T. & Yoshida, M. (2007). *Escherichia coli* phage-shock protein A (PspA) binds to membrane phospholipids and repairs proton leakage of the damaged membranes. *Mol Microbiol* **66**, 100–109.

Lenn, T., Gkekas, C. N., Bernard, L., Engl, C., Jovanovic, G., Buck, M. & Ying, L. (2011). Measuring the stoichiometry of functional PspA

complexes in living bacterial cells by single molecule photobleaching. *Chem Commun (Camb)* **47**, 400–402.

Lima, S., Guo, M. S., Chaba, R., Gross, C. A. & Sauer, R. T. (2013). Dual molecular signals mediate the bacterial response to outer-membrane stress. *Science* **340**, 837–841.

Lloyd, L. J., Jones, S. E., Jovanovic, G., Gyaneshwar, P., Rolfe, M. D., Thompson, A., Hinton, J. C. & Buck, M. (2004). Identification of a new member of the phage shock protein response in *Escherichia coli*, the phage shock protein G (PspG). *J Biol Chem* **279**, 55707–55714.

López, D. & Kolter, R. (2010). Functional microdomains in bacterial membranes. *Genes Dev* **24**, 1893–1902.

Mehner, D., Osadnik, H., Lünsdorf, H. & Brüser, T. (2012). The Tat system for membrane translocation of folded proteins recruits the membrane-stabilizing Psp machinery in *Escherichia coli*. *J Biol Chem* **287**, 27834–27842.

Mehta, P., Jovanovic, G., Lenn, T., Bruckbauer, A., Engl, C., Ying, L. & Buck, M. (2013). Dynamics and stoichiometry of a regulated enhancer-binding protein in live *Escherichia coli* cells. *Nature Commun* **4**, 1997.

Miller, J. H. (1992). *A Short Course in Bacterial Genetics: a Laboratory Manual and Handbook for Escherichia coli and Related Bacteria*. Cold Spring Harbor, NY: Cold Spring Harbor Laboratory.

Model, P., Jovanovic, G. & Dworkin, J. (1997). The *Escherichia coli* phage-shock-protein (*psp*) operon. *Mol Microbiol* **24**, 255–261.

Olshausen, P. v.,, Defeu Soufo, H. J., Wicker, K., Heintzmann, R., Graumann, P. L. & Rohrbach, A. (2013). Superresolution imaging of dynamic MreB filaments in *B. subtilis* – a multiple-motor-driven transport? *Biophys J* **105**, 1171–1181.

Peck, J. W., Bowden, E. T. & Burbelo, P. D. (2004). Structure and function of human Vps20 and Snf7 proteins. *Biochem J* **377**, 693–700.

Raetz, C. R. H. (1986). Molecular genetics of membrane phospholipid synthesis. *Annu Rev Genet* **20**, 253–291.

Renner, L. D. & Weibel, D. B. (2011). Cardiolipin microdomains localize to negatively curved regions of *Escherichia coli* membranes. *Proc Natl Acad Sci U S A* **108**, 6264–6269.

Salje, J., van den Ent, F., de Boer, P. & Löwe, J. (2011). Direct membrane binding by bacterial actin MreB. *Mol Cell* **43**, 478–487.

Takahashi, H., Morioka, R., Ito, R., Oshima, T., Altaf-Ul-Amin, M., Ogasawara, N. & Kanaya, S. (2011). Dynamics of time-lagged gene-to-metabolite networks of *Escherichia coli* elucidated by integrative omics approach. *OMICS* **15**, 15–23.

Tan, B. K., Bogdanov, M., Zhao, J., Dowhan, W., Raetz, C. R. H. & Guan, Z. (2012). Discovery of a cardiolipin synthase utilizing phosphatidylethanolamine and phosphatidylglycerol as substrates. *Proc Natl Acad Sci U S A* **109**, 16504–16509.

Toni, T., Jovanovic, G., Huvet, M., Buck, M. & Stumpf, M. P. H. (2011). From qualitative data to quantitative models: analysis of the phage shock protein stress response in *Escherichia coli*. *BMC Syst Biol* **5**, 69.

Typas, A., Banzhaf, M., Gross, C. A. & Vollmer, W. (2012). From the regulation of peptidoglycan synthesis to bacterial growth and morphology. *Nat Rev Microbiol* **10**, 123–136.

van den Ent, F., Johnson, C. M., Persons, L., de Boer, P. & Löwe, J. (2010). Bacterial actin MreB assembles in complex with cell shape protein RodZ. *EMBO J* **29**, 1081–1090.

van Teeffelen, S., Wang, S., Furchtgott, L., Huang, K. C., Wingreen, N. S., Shaevitz, J. W. & Gitai, Z. (2011). The bacterial actin MreB rotates, and rotation depends on cell-wall assembly. *Proc Natl Acad Sci U S A* **108**, 15822–15827.

Vega, N. M., Allison, K. R., Samuels, A. N., Klempner, M. S. & Collins, J. J. (2013). *Salmonella typhimurium* intercepts *Escherichia coli* signaling to enhance antibiotic tolerance. *Proc Natl Acad Sci U S A* **110**, 14420–14425.

Vothknecht, U. C., Otters, S., Hennig, R. & Schneider, D. (2012). Vipp1: a very important protein in plastids?! *J Exp Bot* **63**, 1699–1712.

Vrancken, K., De Keersmaeker, S., Geukens, N., Lammertyn, E., Anné, J. & Van Mellaert, L. (2007). *pspA* overexpression in *Streptomyces lividans* improves both Sec- and Tat-dependent protein secretion. *Appl Microbiol Biotechnol* **73**, 1150–1157.

Wallrodt, I., Jelsbak, L., Thomsen, L. E., Brix, L., Lemire, S., Gautier, L., Nielsen, D. S., Jovanovic, G., Buck, M. & Olsen, J. E. (2014). Removal of the phage-shock protein PspB causes reduction of virulence in *Salmonella enterica* serovar Typhimurium independently of NRAMP1. *J Med Microbiol* **63**, 788–795.

Wang, P., Kuhn, A. & Dalbey, R. E. (2010). Global change of gene expression and cell physiology in YidC-depleted *Escherichia coli*. *J Bacteriol* **192**, 2193–2209.

Wells, R. C. & Hill, R. B. (2011). The cytosolic domain of Fis1 binds and reversibly clusters lipid vesicles. *PLoS ONE* **6**, e21384.

Westphal, S., Heins, L., Soll, J. & Vothknecht, U. C. (2001). *Vipp1* deletion mutant of *Synechocystis*: a connection between bacterial phage shock and thylakoid biogenesis? *Proc Natl Acad Sci U S A* **98**, 4243–4248.

White, C. L., Kitich, A. & Gober, J. W. (2010). Positioning cell wall synthetic complexes by the bacterial morphogenetic proteins MreB and MreD. *Mol Microbiol* **76**, 616–633.

White, M. J., Savaryn, J. P., Bretl, D. J., He, H., Penoske, R. M., Terhune, S. S. & Zahrt, T. C. (2011). The HtrA-like serine protease PepD interacts with and modulates the *Mycobacterium tuberculosis* 35-kDa antigen outer envelope protein. *PLoS ONE* **6**, e18175.

Wickström, D., Wagner, S., Baars, L., Ytterberg, A. J., Klepsch, M., van Wijk, K. J., Luirink, J. & de Gier, J.-W. (2011). Consequences of depletion of the signal recognition particle in *Escherichia coli*. *J Biol Chem* **286**, 4598–4609.

Yamaguchi, S. & Darwin, A. J. (2012). Recent findings about the *Yersinia enterocolitica* phage shock protein response. *J Microbiol* **50**, 1–7.

Yamaguchi, S., Gueguen, E., Horstman, N. K. & Darwin, A. J. (2010). Membrane association of PspA depends on activation of the phage-shock-protein response in *Yersinia enterocolitica*. *Mol Microbiol* **78**, 429–443.

Yamaguchi, S., Reid, D. A., Rothenberg, E. & Darwin, A. J. (2013). Changes in Psp protein binding partners, localization and behaviour upon activation of the *Yersinia enterocolitica* phage shock protein response. *Mol Microbiol* **87**, 656–671.

Young, B. P., Shin, J. J. H., Orij, R., Chao, J. T., Li, S. C., Guan, X. L., Khong, A., Jan, E., Wenk, M. R. & other authors (2010). Phosphatidic acid is a pH biosensor that links membrane biogenesis to metabolism. *Science* **329**, 1085–1088.

Zhang, L. & Sakamoto, W. (2013). Possible function of VIPP1 in thylakoids: protection but not formation? *Plant Signal Behav* **8**, e22860.

Zhang, L., Kato, Y., Otters, S., Vothknecht, U. C. & Sakamoto, W. (2012). Essential role of VIPP1 in chloroplast envelope maintenance in *Arabidopsis*. *Plant Cell* **24**, 3695–3707.

Zhang, N., Simpson, T., Lawton, E., Uzdavinys, P., Joly, N., Burrows, P. & Buck, M. (2013). A key hydrophobic patch identified in an AAA? protein essential for its *in trans* inhibitory regulation. *J Mol Biol* **425**, 2656–2669.

Edited by: K. Flardh